Molecular Therapy
Methods & Clinical Development
Original Article

Cell therapy with hiPSC-derived RPE cells and RPCs prevents visual function loss in a rat model of retinal degeneration

Anna Salas,[1] Anna Duarri,[1,2,3] Laura Fontrodona,[1] Diana Mora Ramírez,[1] Anna Badia,[1] Helena Isla-Magrané,[1] Barbara Ferreira-de-Souza,[1] Miguel Ángel Zapata,[1] Ángel Raya,[2,4,5] Anna Veiga,[2,3] and José García-Arumí[1,6,7]

[1]Ophthalmology Research Group, Vall d'Hebron Institut de Recerca (VHIR), Vall d'Hebron Hospital Universitari, 08035 Barcelona, Spain; [2]Barcelona Stem Cell Bank, Regenerative Medicine Program, IDIBELL, 08908 Hospitalet de Llobregat, Spain; [3]National Stem Cell Bank-Barcelona Node, Biomolecular and Bioinformatics Resources Platform PRB2, ISCIII, 08908 Hospitalet de Llobregat, Spain; [4]Catalan Institute for Research and Advanced Studies (ICREA), 08010 Barcelona, Spain; [5]Networking Center of Biomedical Research in Bioengineering, Biomaterials and Nanomedicine (CIBER-BBN), 28029 Madrid, Spain; [6]Department of Ophthalmology, Vall d'Hebron Hospital Universitari, Vall d'Hebron Barcelona Hospital Campus, 08036 Barcelona, Spain; [7]Department of Ophthalmology, Autonomous University of Barcelona, 08193 Bellaterra, Spain

Photoreceptor loss is the principal cause of blindness in retinal degenerative diseases (RDDs). Whereas some therapies exist for early stages of RDDs, no effective treatment is currently available for later stages, and once photoreceptors are lost, the only option to rescue vision is cell transplantation. With the use of the Royal College of Surgeons (RCS) rat model of retinal degeneration, we sought to determine whether combined transplantation of human-induced pluripotent stem cell (hiPSC)-derived retinal precursor cells (RPCs) and retinal pigment epithelial (RPE) cells was superior to RPE or RPC transplantation alone in preserving retinal from degeneration. hiPSC-derived RPCs and RPE cells expressing (GFP) were transplanted into the subretinal space of rats. *In vivo* monitoring showed that grafted cells survived 12 weeks in the subretinal space, and rats treated with RPE + RPC therapy exhibited better conservation of the outer nuclear layer (ONL) and visual response than RPE-treated or RPC-treated rats. Transplanted RPE cells integrated in the host RPE layer, whereas RPC mostly remained in the subretinal space, although a limited number of cells integrated in the ONL. In conclusion, the combined transplantation of hiPSC-derived RPE and RPCs is a potentially superior therapeutic approach to protect retina from degeneration in RDDs.

INTRODUCTION

Retinal degenerative diseases (RDDs) are a heterogeneous group of pathologies characterized by the progressive degeneration of photoreceptors (PRs), ultimately leading to blindness,[1] and affect 285 million people worldwide.

Cone and rod photoreceptors are the light-sensing cells in the retina and are responsible for visual input.[2] In close association with the photoreceptors, the retinal pigment epithelium (RPE) provides them several crucial supporting functions, including: recycling of all-*trans* retinol to 11-*cis* retinal in the visual cycle, phagocytosis of photoreceptor outer segments (POS), or light absorption, among others.[3] Photoreceptor loss in RDDs may be the result of photoreceptor dysfunction or may result from RPE loss or dysfunction. Nowadays, treatment strategies are mainly focused on the early stages of the diseases, preventing retinal degeneration through neuroprotection and gene therapies. To date, there is no effective treatment capable to revert cell death and restore visual function in later stages; thus, research in cell-based therapies for retina regeneration has been the subject of intense investigation.

Mammalian retinas have limited regenerative capacity,[4] and cell-based therapies aiming to restore light sensitivity are highly desirable. Human pluripotent stem cells (hPSCs), both embryonic (hESC) or induced (hiPSC), can differentiate into any retinal cell type and can thus serve as a renewable cell source to repair degenerated retinas.[5,6] In this context, hESC-derived RPE cell transplantation has been successful in several preclinical models,[6] although long-term efficacy has yet to be defined. Likewise, several clinical trials in age-related macular degeneration (AMD), retinitis pigmentosa, and Stargardt's disease have been proven safe but with only limited improvements in vision.[7–10] These results likely suggest that at later disease stages, when photoreceptors have degenerated, transplanted RPE cells are unable to rescue vision, since they are not light sensing cells. Thus, several photoreceptor-replacement therapies have been explored to overcome this limitation, including full-thickness retinal patches,[11–14] retinal progenitor cells,[15–17] neural progenitor cells,[18,19] and stem

Received 1 July 2020; accepted 4 February 2021;
https://doi.org/10.1016/j.omtm.2021.02.006.

Correspondence: Anna Duarri, PhD, Ophthalmology Research Group, Vall d'Hebron Institut de Recerca, Vall d'Hebron Hospital Universitari, Passeig de la Vall d'Hebron 119-129, Collserola Building, Laboratory 148, 08035 Barcelona, Spain.
E-mail: anna.duarri@vhir.org

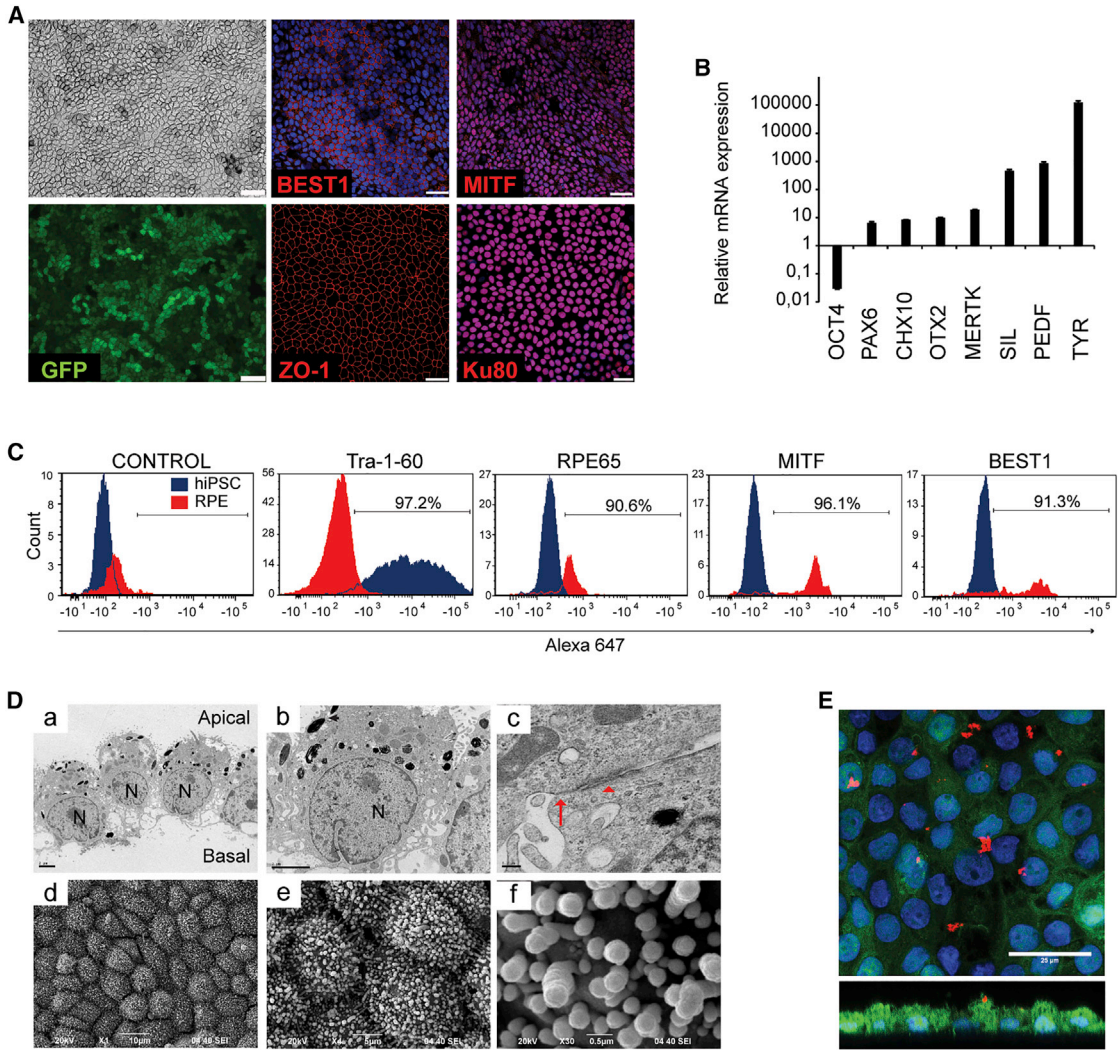

Figure 1. Characterization of human-induced pluripotent stem cell (hiPSC)-derived retinal pigment epithelium (RPE) cells

(A) RPE-like cells exhibited typical pigmented hexagonal cell morphology under bright-field and expressed green fluorescent protein (GFP). Representative immunostaining images show expression of RPE markers bestrophin-1 (BEST1), ZO-1 (*zonula occludens* 1), MITF (microphthalmia-associated transcription factor), and a human antigen (Ku80). Nuclei are stained with DAPI. Scale bars, 75 μm in left panels and 50 μm in middle and right panels. (B) Gene-expression levels in RPE-like cells by quantitative real-time PCR. Values are normalized to *GAPDH* and relative to undifferentiated hiPSC, expressed as $2^{-\Delta\Delta Ct}$ (log scale). Data presented as mean ± standard deviation (SD; n = 3), five independent biological replicates. (C) Quantitative analysis by flow cytometry of RPE65, MITF, and BEST1 in RPE cell culture. Histograms show both the undifferentiated hiPSC (blue) and RPE cells (red). Results are representative of two independent experiments performed with cells from different differentiations. (D) Representative transmission electron microscopy (TEM; a–c) and scanning electron microscopy (SEM; d–f) images of RPE cells in culture. RPE monolayers show polarization with apical microvilli, melanosomes, mitochondria, tight junction (red arrow), and adherent junction (red arrowhead) at the apical border and basal nuclei (N). Scale bars, 2 μm (a and b) and 0.2 μm (c) for TME images. Scale bars, 10 μm (d), 5 μm (e), and 0.5 μm (f) for SEM images. (E) *In vitro* phagocytosis of tetramethylrhodamine (TRITC)-labeled photoreceptor (PR) outer segments (POS; red) by RPE-like cells (GFP in green). Nuclei are stained with DAPI. Scale bar, 25 μm.

cell-derived retinal progenitors,[20–34] which have been proven to restore visual function in animal models of photoreceptor dysfunction. The majority of cell replacement strategies are currently based on transplantation of a single cell-type rather than multiple cell types; however, in the setting of defective RPE, transplantation of photoreceptors only might not be sufficient without a healthy RPE support. In that case, selective replacement of both RPE and photoreceptor cell types might be a better strategy to regenerate the retinas.

The Royal College of Surgeons (RCS) rat model of autosomal-recessive retinitis pigmentosa has been extensively used for cell therapeutic approaches, since it is a good model for developing cell therapies focused on severe retinopathies. RCS rats carry a defective *MERTK* gene,[35] a receptor tyrosine kinase expressed in RPE cells, which leads to RPE malfunction of phagocytosis of POS that in turn trigger severe photoreceptor cell death, beginning at 3 weeks after birth and continuing rapidly over 4 weeks.[36,37] We previously demonstrated

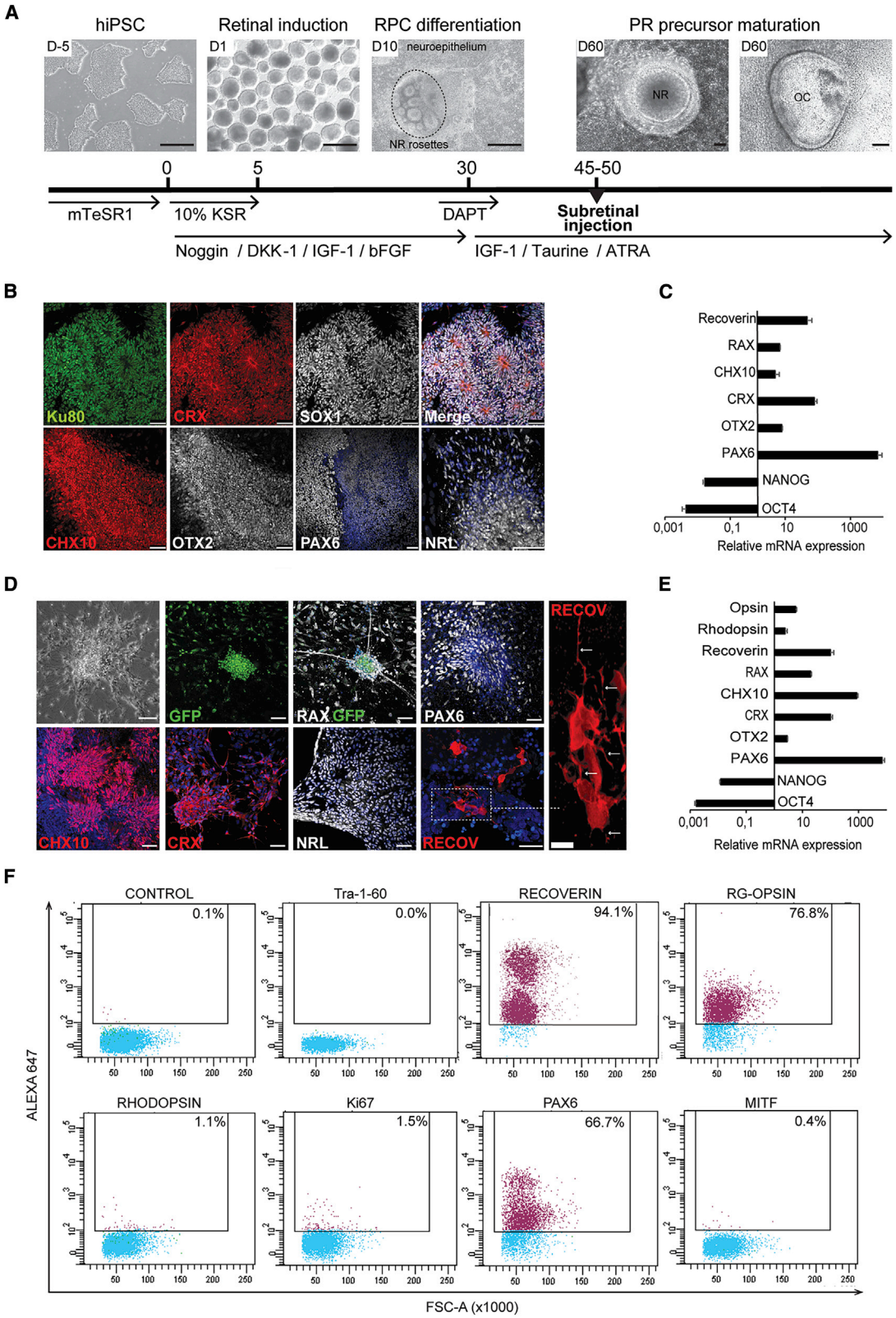

(legend on next page)

the potential of hESC and hiPSC to generate transplantable RPE cells, but these cells failed to exert significant long-term improvement of visual function.[38] In the current study, we developed a protocol to generate both retinal precursor cells (RPCs), consisting mainly in photoreceptor precursor cells, and RPE cells from hiPSC. Our main objective was to assess whether a cell-transplantation strategy using a combination of RPE cells and RPC would be superior to RPE or RPC therapies alone using the RCS rat model and to explore the potential of our RPC to integrate and repopulate the degenerative endogenous photoreceptor layer.

RESULTS

Differentiation and characterization of RPE-like cells derived from hiPSCs

Previously, we successfully differentiated hESCs and hiPSCs to RPE-like cells.[38] With the use of the same protocol here, we obtained a homogeneous culture of RPE cells recapitulating the native cellular morphology, including a characteristic pigmented polygonal cell shape (Figure 1A). To facilitate *in vivo* detection of transplanted cells, we transduced RPE cells with lentiviral particles carrying a GFP reporter gene. RPE cells in culture constitutively expressed GFP and the human nuclear antigen Ku80 (Figure 1A). RPE cells also expressed specific early ocular markers, including *PAX6*, *OTX2*, MITF, and *CHX10*, and the mature RPE markers bestrophin-1, RPE65, ZO-1, *SIL*, *PEDF*, *MERTK*, and *TYR* and showed downregulation of *OCT4* and Tra-1-60 (Figures 1A–1C). Along maturation, the RPE cell monolayer polarized and acquired apical-basolateral specialization, columnar-shape morphology with apical melanin-containing melanosomes and tight junctions, as observed by transmission electron microscopy (TEM) (Figure 1D, a–c). Microvilli were also observed in the apical side by scanning electron microscopy (SEM) (Figure 1D, d–f). As RCS rats carry a defective *mertk* gene, which is essential for RPE to phagocytize POS, we ensured that the hiPSC-derived RPE cells exhibited native phagocytic function before transplantation, as demonstrated by their internalization of tetramethylrhodamine (TRITC)-labeled POS *in vitro* (Figure 1E). Overall, these results show that the RPE cell-differentiation protocol is robust, reproducible, and generates functional RPE-like cells.

Differentiation and characterization of RPCs derived from hiPSCs

To guide hiPSCs to the retinal lineage, we used a differentiation protocol based on a previous study (Figure 2A).[39] Upon neuroretina induction, embryoid bodies (EBs) were seeded onto Matrigel to develop an anterior neuroepithelium, followed by neural rosette formation observed by day 7. Early neural retina and optic cups were apparent by day 25 of culture and showed signs of internal lamination surrounded by a few pigmented cells at day 60 of differentiation (Figure 2A). We characterized retinal cells at different time points by immunocytochemistry, qRT-PCRquantitative real-time PCR, and flow cytometry. At day 21 of differentiation, cell culture comprised retinal progenitor cells that formed neural rosettes and neuroepithelium (Figure 2B). Retinal progenitors expressed the early-stage-specific markers PAX6, RAX, CHX10, and OTX2 and the photoreceptor progenitor markers CRX, recoverin, and NLR and showed a decrease in the expression of the pluripotency genes *OCT4*, *NANOG*, and Tra-1-60 (Figures 2B and 2C; Figure S1A). At this stage, retinal progenitors were proliferative (Ki67+), as it is shown by flow cytometry (Figure S1A). At days 45–50, cell culture was composed of a homogeneous population of more mature retinal cells, hereinafter RPCs, which along with GFP (cells transduced with lentivirus before transplantation), RAX, CHX10, and PAX6, together with CRX and NRL expression, we detected cell clusters containing recoverin + cells (Figures 2D–2F). Within RPC cultures, recoverin + photoreceptor precursors had extended axonal projections (arrows in magnification; Figure 2D). Furthermore, we could detect expression of *OPSIN* and *RHODOPSIN* transcripts by quantitative real-time PCR (Figure 2E), similar to another study.[34] Flow cytometry analysis revealed that the RPC mostly expressed recoverin, red/green coneopsin (RG-OPSIN), and PAX6, whereas a smaller proportion (1.1%) expressed rhodopsin (Figure 2F). The manifestation of pigmented foci in our cultures, corresponding to RPE cells, was observed from day 30, although the percentage of pigmented RPE was relatively low, as demonstrated by flow cytometry at day 45 with only 0.4% of total cells. Moreover, RPC at day 45 was not mitotically active, as it is shown by the low Ki67 levels (1.5%) (Figure 2F). At day 90 of differentiation, retinal cell cultures showed mature photoreceptor cells expressing CRX, recoverin rhodopsin, and RG-opsin, and these cells also presented longer axonal projections

Figure 2. Generation and characterization of retinal precursor cells (RPCs) from hiPSCs

(A) Schematic diagram of the three-step protocol at different stages of differentiation. Bright-field images of cell morphology of undifferentiated hiPSC colonies at day −5, embryoid bodies at day 1, early retinal rosettes containing RPCs at day 10, and optic cup-like structures at day 60. Scale bars, 500 μm and 100 μm. (B) At day 21, confocal images of retinal progenitor cells forming neural rosettes and expressing human antigen Ku80; eye-field primordial and neural retina markers SOX1, CHX10, OTX2, and PAX6; and early PR markers CRX and NRL. Scale bars, 50 μm. (C) Quantitative real-time PCR of gene expression at day 21 relative to undifferentiated hiPSC shows downregulation of pluripotent genes *OCT4* and *NANOG* and upregulation of neural (*PAX6*, *OTX2*, and *CHX10*) and photoreceptor (*CRX*, *RAX*, and *recoverin* [Recov]) genes. Values are normalized to *GAPDH* and relative to undifferentiated hiPSC, expressed as $2^{-\Delta\Delta Ct}$ (log scale). Data presented as mean ± SD (n = 3), three independent biological replicates. (D) Representative bright-field and immunocytochemistry images of RPC cultures transduced with the lentivirus SparQ-GFP at day 45 (before transplantation). The expression of GFP, neural retina marker (CHX10, PAX6, and RAX), and PR progenitor markers (NRL, RECOV, and CRX) is shown. Magnification of Recov + cells with axonal projections (white arrows). Scale bars, 75 μm (bright field); 50 μm and 10 μm in the magnifications. Nuclei are stained with DAPI. (E) uantitative real-time PCR of gene expression in RPCs at day 45 relative to undifferentiated hiPSC shows no expression of pluripotent genes (*NANOG* and *OCT4*) but upregulation of retinal markers, including mature PR markers *opsin* and *rhodopsin*. Values are normalized to *GAPDH* and relative to undifferentiated hiPSC, expressed as $2^{-\Delta\Delta Ct}$ (log scale). Data presented as mean ± SD (n = 3), three independent biological replicates. (F) Quantitative flow cytometry analysis of RPC at day 45 with surface marker Tra-1-60 and intracellular markers RECOV, RHO, RG-OPSIN, and PAX6 (specific for RPC), MITF (for RPE cells), and Ki67 (proliferation) and the appropriate controls (undifferentiated hiPSC, retinal progenitors at day 21, and secondary antibody are shown in Figure S1). The numbers in the corner show the percentage of stained cells in this gate. Secondary antibody was used as control. Results are representative of two biological replicates.

Table 1. Groups of transplanted RCS rats at postnatal days 21–24

Experiment	Treatment (cell suspension injection)	No. of injected cells	No. of rats	No. of successfully injected eyes	Successful injection rates
#1	RPE	10^5	13	20	77%
	RPE + RP d21	$5 \times 10^4 + 5 \times 10^4$	20	34	85%
	RPE + RPC d45–50	$5 \times 10^4 + 5 \times 10^4$	20	13	64%
	RPE + RPC d75	$5 \times 10^4 + 5 \times 10^4$	17	28	82%
	Sham	–	15	21	70%
#2	RPE	10^5	20	30	75%
	RPE + RPC d45–50	$5 \times 10^4 + 5 \times 10^4$	23	32	70%
	RPC d45–50	10^5	8	11	68%
	Sham	–	10	15	75%

RPE, retinal pigment epithelium; RP, retinal progenitor; RPC, retinal precursor cell; d21, day 21 of differentiation; d45–50, days between 45 and 50 of differentiation; d75, day 75 of differentiation.

as compared with day 45 (Figure S1B) This indicated that our protocol enriches for a population of RG cone photoreceptors.

Establishing the optimal RPC developmental time window for transplantation

Studies have shown that the maturity of stem cell-derived photoreceptors is key for successful engraftment, maturation, and function in the correct host retinal layer.[24,28] Thus, we first determined the best retinal cells' differentiation time window to improve retinal conservation and visual function recovery in the RCS model. In a pilot study (Table 1, experiment 1), we cotransplanted hiPSC-derived RPE cells together with retinal progenitors at day 21, RPC at days 45−50, and more mature RPC at day 75; RPE cells alone; or medium (sham) into the subretinal space of RCS rats at postnatal days between 21 and 24, corresponding to the initial stages of photoreceptor degeneration. We then analyzed visual function by electroretinography (ERG) and retina conservation by histology at 8 and 12 weeks post-transplantation (Figure S2). Cotransplantation of RPE + RPC at days 45–50 and day 75 of differentiation led to a significant preservation of visual function at 12 weeks compared with RPE-transplanted rats and the sham group ($p < 0.05$) and was superior to that in retinas transplanted with RPE + retinal progenitors at day 21 (Figures S2A−S2C). We also observed a better preservation of the outer nuclear layer (ONL) from 8 to 12 weeks with RPE + RPC differentiated for 45–50 days or for 75 days when compared with RPE + retinal progenitors differentiated for 21 days, RPE cells alone, or sham (Figure S2D). These data suggest that day 21 differentiated retinal progenitor cultures consist of immature progenitors that fail to preserve or improve retinal function and that RPC days 45–75 cultures consist of precursor cells at an equivalent stage of development to those of RCS rats. Based on these results, we established our transplantable developmental time window at days 45–50.

Transplanted RPE + RPCs survive in the subretinal space of RCS rats and can be monitored *in vivo* over 12 weeks

In a second experiment, we performed a comprehensive study of the progression, survival, and integration of transplanted cells in the RCS model (Table 1; experiment 2). Four groups of RCS rats were subretinally injected with cell suspensions of RPE cells, RPC cells at days 45–50 of differentiation, a combination of RPE cells and RPC, or medium. All transplanted cells expressed GFP, and the injected eyes were periodically monitored by fluorescence fundus imaging (FFI) and optical coherence tomography (OCT) for 12 weeks. We first followed the presence and evolution of cell grafts in the host retinas (Figure 3). In all groups, retinas appeared detached and formed a subretinal bleb (Figures 3A−3C, a and b) containing the injected cell suspension. 1 week after injection, the bleb was absorbed, and cell grafts were detected as fluorescent dots randomly distributed around the injection area (Figures 3A−3C, c and d). 2 weeks postinjection, retinas had almost recovered their natural position, and the fluorescent clumps seemed to be partially reduced in size (Figures 3A−3C, e and f). The level of fluorescence remained very similar from 4 to 12 weeks in the RPE + RPC group, indicating the survival of most of the cells present at week 2 (Figure 3C, g−l). However, the fluorescent cell grafts in the RPE and the RPC groups were reduced drastically from 4 weeks after transplantation (Figures 3A and 3B, g and h), and very few green cells were observed at 12 weeks (Figures 3A and B, k and l) even though rats were under immunosuppression, stating the difficulty of RPE or RPC survival when transferred alone in the retina of the RCS model.

Combined RPE + RPC therapy induces a better survival of endogenous photoreceptors than RPC or RPE cell therapies

The RCS rat model is primarily characterized by severe degeneration of photoreceptors as a consequence of the RPE cell dysfunction, which can be easily observed by OCT at postnatal day 60.[40] To evaluate whether RPE + RPC, RPC, or RPE cell therapies could rescue photoreceptor degeneration, we examined the total retina thickness and the photoreceptor layer thickness (consisting of ONL + outer and inner photoreceptor segments) in all groups. Quantifications were performed at 4 weeks (Figures 4A−4F), 8 weeks (Figures 4G−4L), and 12 weeks (Figures 4M−4R) postinjection, and retinal preservation of the grafted area was normalized by the thickness of the contralateral area of the same eye and compared between groups.

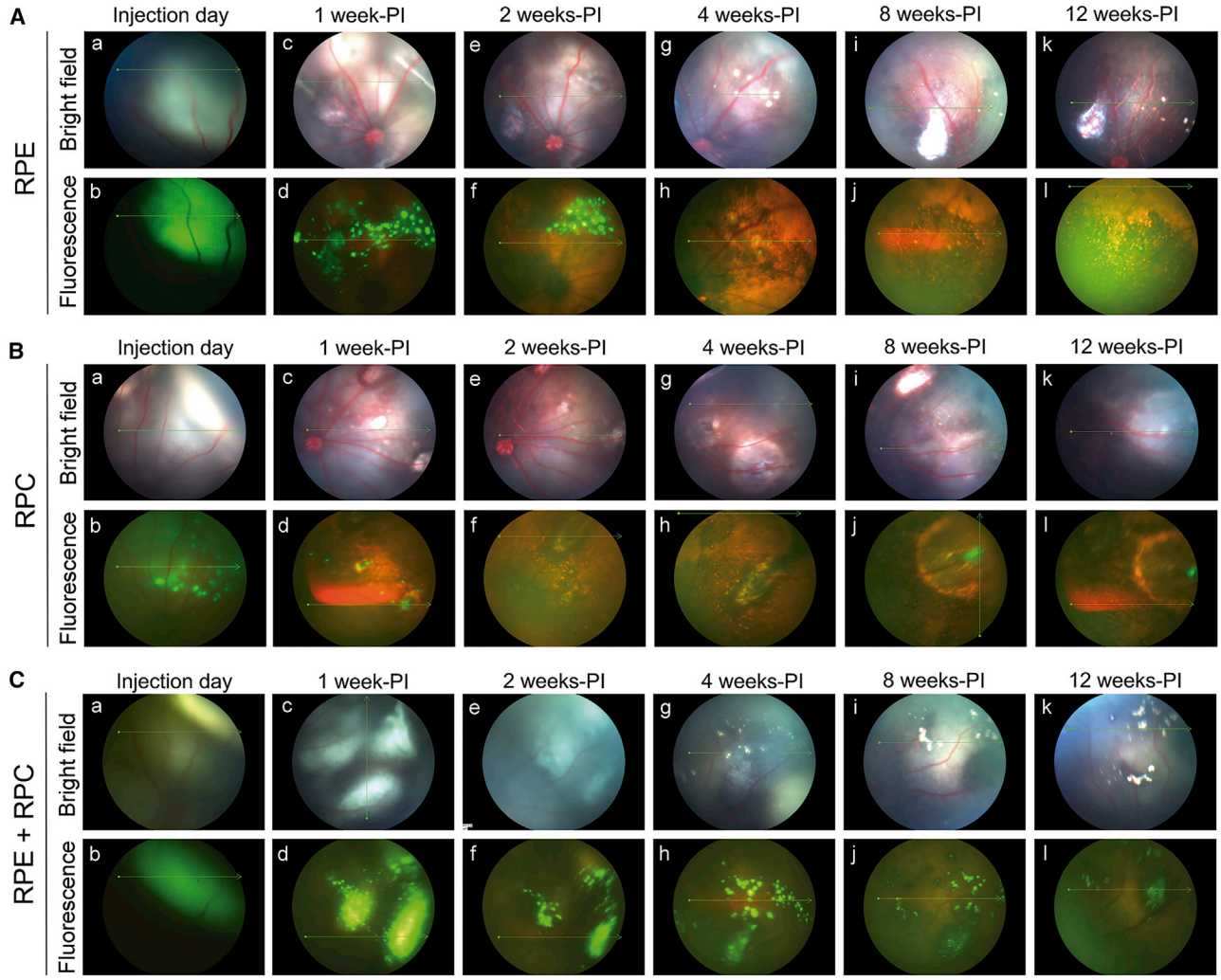

Figure 3. *In vivo* time course of GFP-fluorescent cell survival in the subretinal space of the RCS rat

(A) Images from the same eye injected with RPE cells alone at 1, 2, 4, 8, and 12 weeks postinjection (PI). (B) Images from the same eye injected with RPC alone. (C) Images from the same eye injected with the combination of RPE + RPC alone. Images show fundus retinographies (a, c, e, g, i, and k) and fluorescent retinographies under blue filter (b, d, f, h, j, and l) in the same area, where grafted GFP+ cells are observed as green spots.

At 4 weeks after transplantation, retinal micrographs showed no differences in terms of retina preservation among the four groups (Figure 4E). Conversely, at 8 and 12 weeks postinjection, we observed a significant rescue of the total retina (Figures 4K and 4Q) and photoreceptor layer thickness (Figures 4L and 4R) in the group treated with combined RPE + RPC compared with RPC, RPE, and sham groups. Moreover, at 12 weeks, the RPC group exhibited a marked reduction of both total retina and ONL thickness compared to 8 weeks (Figures 4Q and 4R). Of note, we did not observe any nuclei in the ONL of sham-injected eyes[36] at 12 weeks postinjection, whereas we detected some nuclear layers in RPE-, RPC-, and RPE + RPC-transplanted eyes (Figures 4M–4P). In summary, combined RPE + RPC cell therapy is better at preserving retinas from degeneration than RPE and RPC cell therapies.

Combined RPE + RPC therapy preserves visual function better than RPC or RPE cell therapies alone

We previously showed that RPE transplantation in the subretinal space of RCS rats partially preserved retinal function up to 8 weeks postinjection.[38] To assess whether combined RPE + RPC therapy was superior to RPC or RPE cell transplantation at preserving responses to light stimuli, we compared the electrical response of the different treatment groups by scotopic ERG at 4, 8, and 12 weeks postinjection (Figures 5A–5C). Animals were stimulated with green light from −1.1 to 1.9 log cd · s · m^{-2} to acquire the best retinal response, and ERG waves were analyzed by amplitude and implicit time quantification (Figures 5D–5G). Measurements shown in Figure 4 are those corresponding to 1.9 log cd · s · m^{-2}. At 4 weeks postinjection, ERG responses obtained from RPE and RPE + RPC cell-engrafted

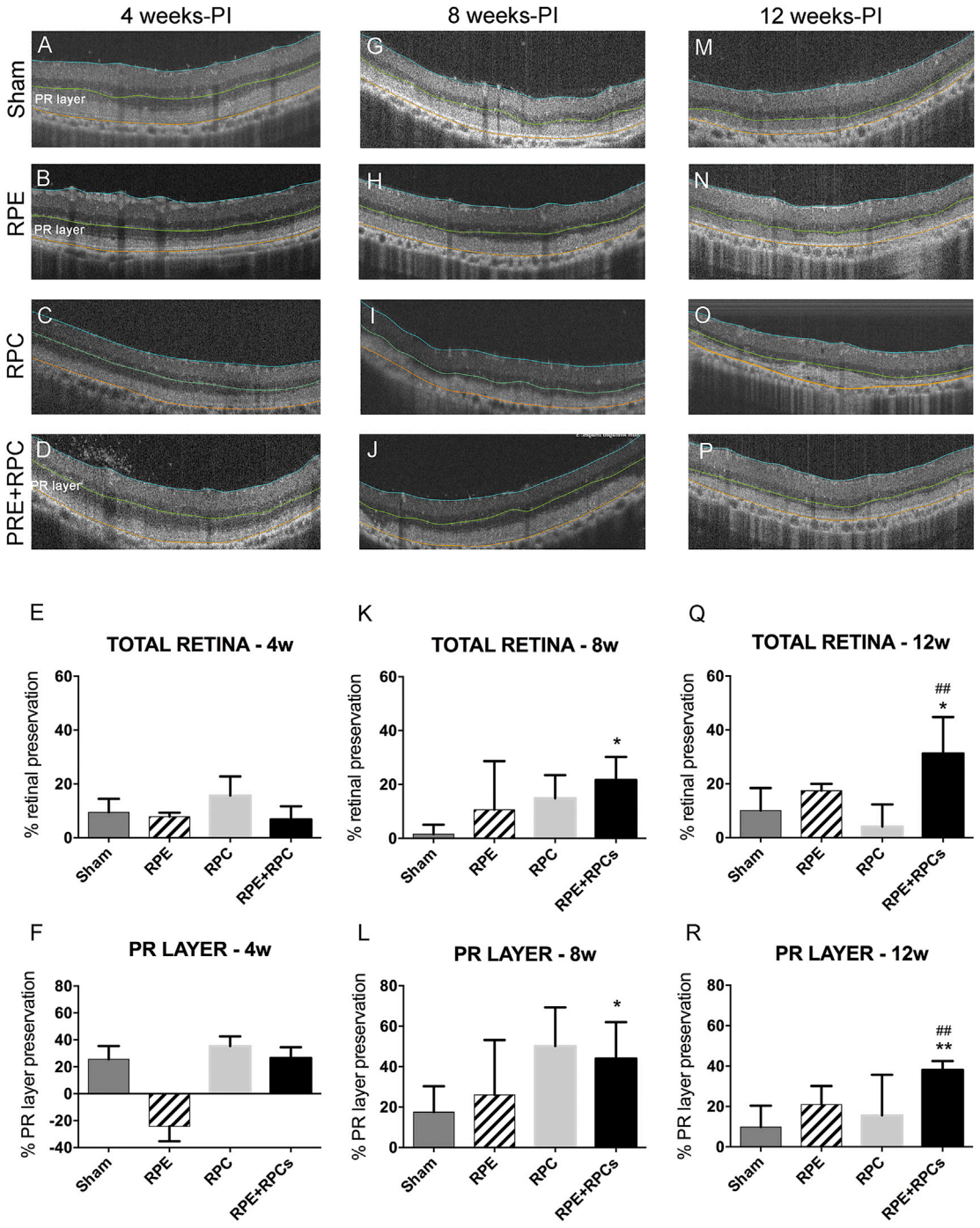

Figure 4. Structural analysis of transplanted retinas by optical coherence tomography (OCT)

Eyes injected with medium (sham; A, G, and M; n = 6 eyes), RPE cells (B, H, and N; n = 8 eyes), RPC (C, I, and O; n = 6 eyes), or the combination of RPE and RPC (RPE + RPCs; D, J, and P; n = 10 eyes) were analyzed at 4, 8, and 12 weeks PI by OCT, obtaining retina micrographs of the grafted area and a contralateral area of the same eye (not shown). Cross-sections of the retinas were analyzed, quantifying total retina thickness (TOTAL RETINA; area between blue and orange lines) and PR layer thickness (PR LAYER; area between green and orange lines). The preservation of the thickness of total retina and PR layer was compared among groups at 4 (E and F), 8 (K and L), and 12 weeks PI (Q and R), calculating the difference between the grafted area and the contralateral area of the same eye. Data presented as mean ± SD. Statistical significance was calculated by one-way ANOVA, followed by Tukey's multiple comparison tests. *$p < 0.05$; **$p < 0.005$ between RPE + RPC and sham groups; #$p < 0.05$; ##$p < 0.005$ between RPE + RPC and RPE groups.

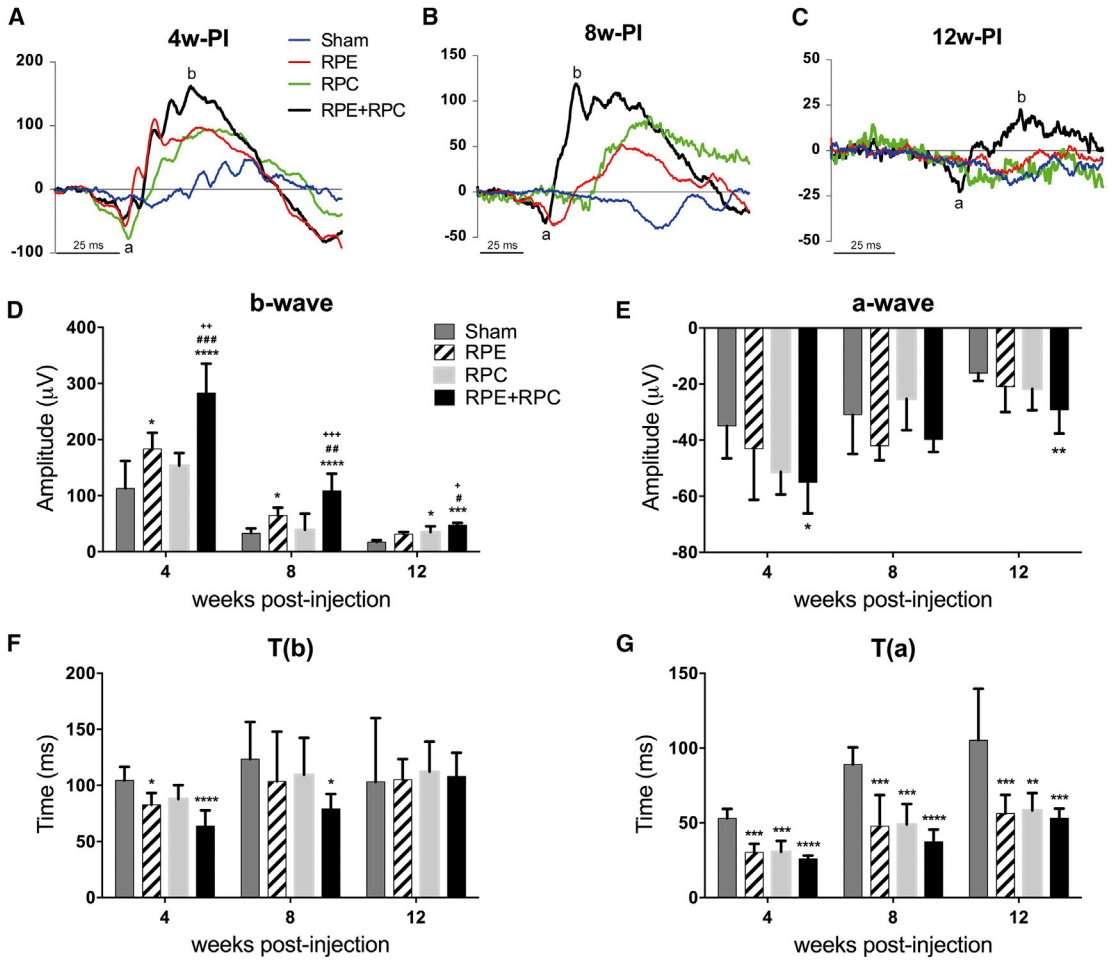

Figure 5. Visual function analysis by electroretinogram

(A–C) Representative electroretinogram recordings at 4, 8, and 12 weeks PI. Scotopic electroretinogram responses were recorded from eyes injected with medium (sham; blue lines, n = 7 eyes), RPE-differentiated cells (RPE; red lines, n = 8 eyes), RPC-differentiated cells (RPC; green lines, n = 8 eyes), or the combination of RPE and RPCs (RPE + RPC; black lines, n = 9 eyes). Measurements were recorded under a light stimulus of 1.9 log cd · s · m^{-2} and 1 ms of duration. (D–G) Electroretinographic waves were quantified and compared among treatment groups at the three time points by the measurement of the b-wave amplitude (D) and its implicit time (F) and the a-wave amplitude (E) and its implicit time (G). Data presented as mean ± SD. Statistical significance was calculated by two-way ANOVA, followed by Tukey's multiple comparison tests comparing sham with RPE, RPC, and RPE + RPC data (*), comparing RPE with RPE + RPC data (#), or comparing RPC with RPE + RPC data (+). *p < 0.05; **p < 0.005; ***p < 0.0005; ****p < 0.0001; #p < 0.05; ##p < 0.005; ###p < 0.0005; +p < 0.05; ++p < 0.005; +++p < 0.0005.

eyes were clearly higher than those obtained from sham-injected eyes, exhibiting a significantly higher b-wave and a significantly shorter implicit time (Figures 5D–5F). However, RPC-engrafted eyes did not produce significantly better ERG signals at 4 weeks. Furthermore, eyes injected with the RPE + RPC combination showed a better b-wave response than eyes injected with RPE and PRC alone (Figure 5D). This significant improvement in the visual function by combined therapy was consistent until 12 weeks postinjection. Nevertheless, the retinal signal of all animals inevitably decreased along this time period, likely due to the progressive retinal neurodegeneration of the model and the effect of immunosuppression with cyclosporin A, which has been shown to reduce visual response in RCS rats.[40] A-wave amplitudes at 4 weeks postinjection were significantly better in the RPE + RPC cell-injected group than in the sham group, and this significance was also observed at 12 weeks postinjection (Figure 5E). In addition, the implicit time of the a-wave was significantly shorter in all of the cell-injected groups compared to the sham group at all three time points assessed, indicating a faster response with the cell therapies (Figure 5G). Overall, the functional results obtained by ERG demonstrate the superiority of the combined RPE + RPC therapy over the RPE and the RPC cell therapies alone in preserving visual function over 12 weeks after transplantation.

RPC and RPE cells integrate in the degenerating rat retina

Consistent with the OCT data, postmortem histological analyses of eyes transplanted with RPE + RPC at 8 and 12 weeks revealed

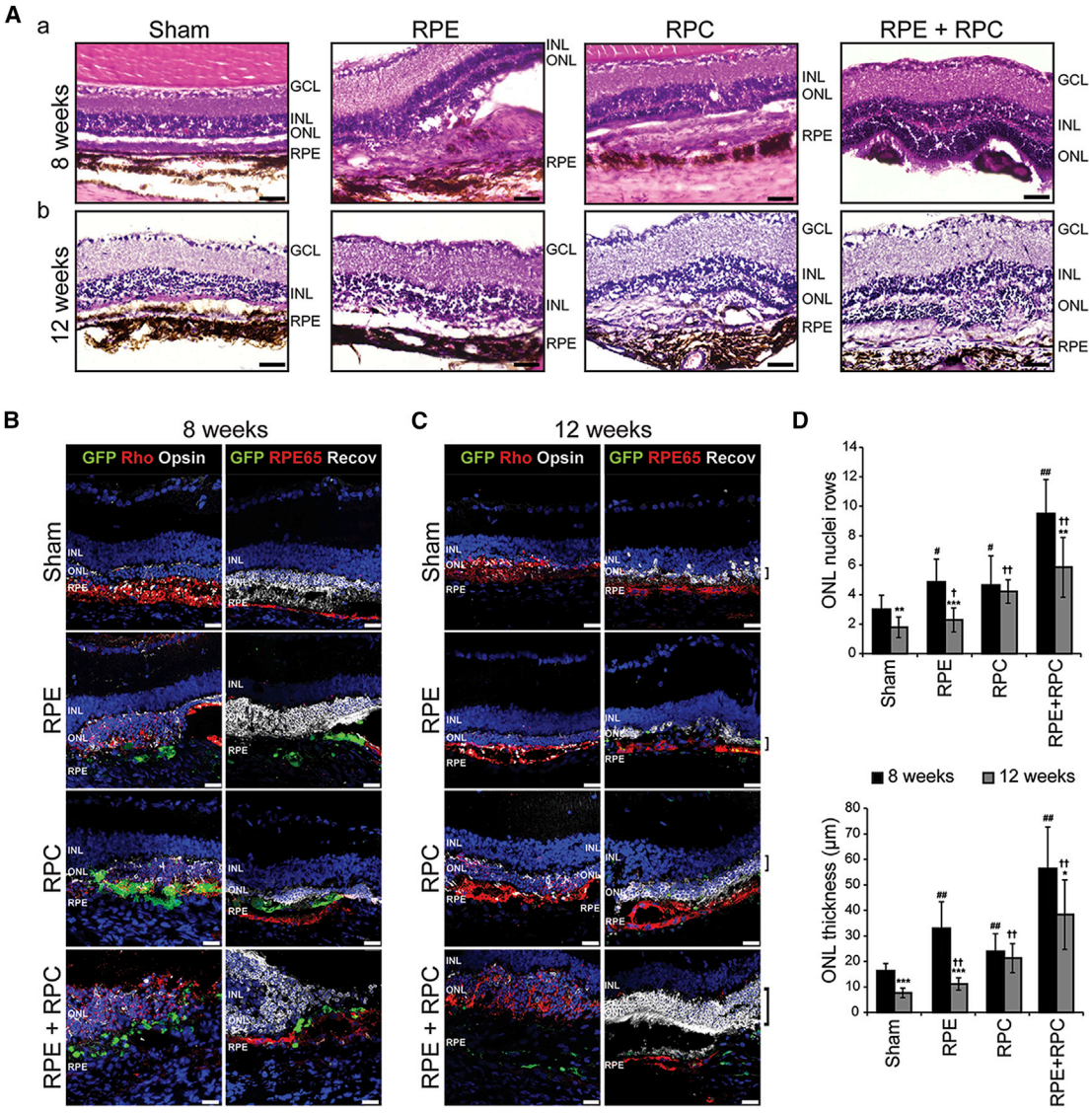

Figure 6. Postmortem analysis of RPE and RPC integration in the RCS rat retina

(A) Hematoxylin and eosin of rat eye cryosections injected with sham (control), RPE cells, RPC, and RPE + RPC at 8 weeks (a) and 12 weeks (b) PI (n = 3 eyes/group). Scale bar, 50 μm. (B) Immunofluorescence analysis of Rho, blue opsin, RPE65, and Recov in sections of RCS rat retinas at 8 weeks PI with sham (control), RPE cells, RPC, and RPE + RPC cell suspensions. Scale bars, 25 μm. (C) Immunofluorescence staining with Rho, blue opsin, RPE65, and Recov in sections of RCS rat retinas at 12 weeks PI with sham (control), RPE, RPC, and RPE + RPC cell suspensions. Brackets indicate outer nuclear layer (ONL). Scale bars, 25 μm. Nuclei were stained with DAPI. (D) Quantification of ONL nuclei rows (top graph) and ONL thickness (bottom graph) in retinal paraffin sections (n = 3–5 eyes/group). Data are expressed as mean ± SD. *p < 0.01; ***p < 0.0005; **p < 0.001 versus 8 weeks; #p < 0.01; ##p < 0.001 versus control at 8 weeks; †p < 0.05; ††p < 0.00001 versus control at 12 weeks, calculated using Student's t test. GCL, ganglion cell layer; INL, inner nuclear layer.

extensive conservation of the photoreceptor layer that extended around the injection site, and this was better compared to that of the eyes transplanted with RPC or RPE cells only (Figure S3A). At 8 weeks postinjection, we observed well-defined engrafted cell clusters containing pigmented cells in both RPE + RPC and RPE cell groups but not in the RPC group (Figure 6A, a). The rescue of the photoreceptor layer was more manifest at 12 weeks postinjection (Figure 6A, b). Flat-mounted RPE layers of eyes injected with RPE + RPC showed that engrafted RPE cells were distributed in GFP+ cell patches, similar to what we observed *in vivo*, and exhibited a regular hexagonal morphology and tight junctions, shown by ZO-1 staining (Figure S3B).

We next assessed the integration of transplanted cells in the host retina. Analysis of the combined RPE + RPC therapy at 1 week postinjection showed that transplanted cells remained in the subretinal

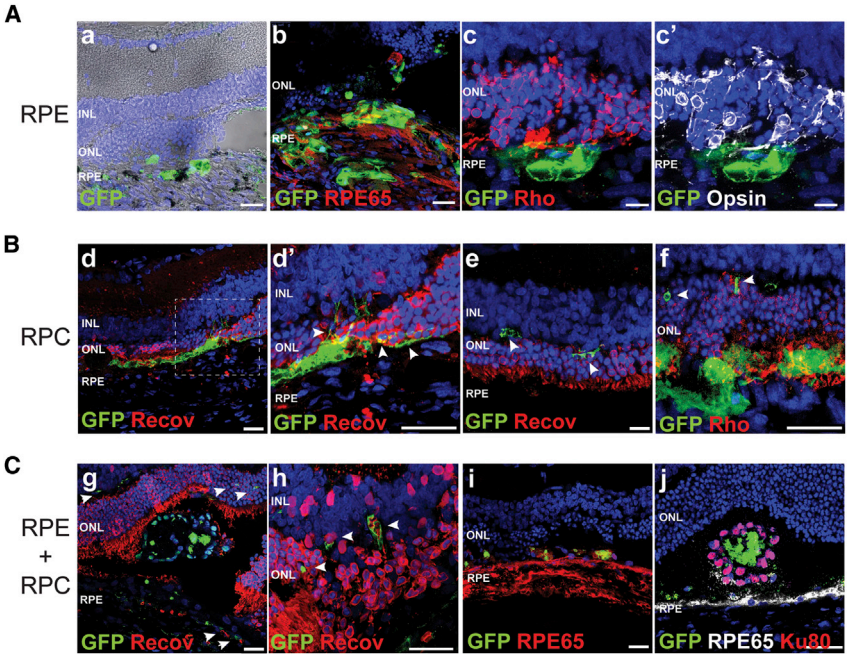

Figure 7. Identification of RPE and RPC engrafted in the RCS rat retina

(A) Immunostaining of retinal sections at 8 weeks PI with RPE showing engraftment of GFP+ RPE cells in the host RPE layer (n = 4 eyes). (a) Bright-field image corresponding to Figure 6B showing pigmented GFP+ RPE cells. (b) GFP+ RPE cells expressed RPE65. (c and c') Costaining with Rho and opsin showing interaction of engrafted GFP+ RPE with endogenous photoreceptors. (B) Immunostaining of retinal sections at 8 weeks PI with RPC showing integration of RPC into the ONL (n = 4 eyes). (d and e) Staining with Recov. White dashed square in (d) indicates the area enlarged in (d'). (f) Magnification of Figure 6B showing that GFP+ RPC expressed Rho. (C) Immunostaining of retinal sections at 8 weeks PI with PRE + RPC (n = 5 eyes). (g–j) Staining with Recov, RPE65, and human antigen Ku80. White arrowheads indicate GFP+ RPC cells integrated to ONL in (d), (e), (f), (g), and (h). GFP+ RPE cells integrate into the host RPE layer as a discrete monolayer (i) or as clusters (g) and (j). Scale bars, 25 μm. GFP in green. Nuclei were stained with DAPI.

space (Figure S4A), evidenced by GFP+ and Ku80+ cells (Figure S4B). Because of the assortment of RPE cells and RPC, some transplanted cells expressed RPE65, and others expressed CRX and opsin, and only a few cells were proliferative (Ki67+), similar to what we observed at 8 weeks (Figure S3C).

Notably, at 8 weeks postinjection, the conservation of the ONL was evident in all cell treatments in the cryosection, as shown by the expression of recoverin, rhodopsin, and opsin (photoreceptor markers) in contrast to sham-injected retinas (Figure 6B). Most of the transplanted RPE cells localized in the RPE layer, expressed RPE65, acquired pigmentation, and interacted with endogenous POS (Figures 6B, 6C, and 7, a, b, c, c', and i). We also observed that GFP+ RPE cells formed clusters in the subretinal space and coexpressed RPE65 and Ku80, with no evidence of nuclei fragmentation (Figure 7, i and j). Most transplanted RPCs remained in the subretinal space (Figures 6B and 6C), but we observed some RPC integrated into the ONL, coexpressing recoverin and extending their projections through the layers (Figure 7, d–h). We also observed that in sham-injected eyes, ONL thickness was reduced and contained less rows of nuclei in the ONL, whereas RPE- and RPC-transplanted retinas maintained similar rows of nuclei and ONL thickness. In contrast, in RPE + RPC-transplanted retinas, ONL was thicker and contained more rows of nuclei (Figure 6D) ($p < 0.001$).

The number of GFP+ cells at 12 weeks postinjection was significantly lower in all cell-transplanted eyes than in equivalent eyes studied at 8 weeks (Figure 6C), which resulted in a progressive reduction of ONL and retinal thickness (Figure 6D). However, the conservation of the ONL was considerably better in the RPE + RPC-treated group, as shown by the expression of rhodopsin, opsin, and recoverin by endogenous photoreceptors (Figure 6C).

It has been described that retinas transplanted with photoreceptor cells expressing fluorescent reporters can exchange cellular material with host cells.[41] In the RPC and combined RPE + RPC groups, we also found some GFP signals in the inner nuclear layer and the ganglion cell layer, probably due to material transfer to neighboring rat cells (Figure S3D), a phenomenon that was not observed in the RPE cell therapy group.

Although RCS rats were immunosuppressed during cell treatments, we observed activated microglia and Müller glial cells in the subretinal space surrounding GFP+ cells, which was more evident in the combined RPE + RPC therapy, as evidenced by Iba1 and glutamine synthetase staining (Figure S5). It is worthy of mention that the retinal degeneration itself also triggered the activation of microglia and Müller glia cell in the subretinal space of sham-injected retinas (Figure S5).

Taken together, these results indicate that although most of the transplanted RPC remained in the subretinal space, the combined RPE + RPC grafts survived longer and better conserved the ONL than RPE- or RPC-only engrafted cells in the 12-week study period.

DISCUSSION

As part of our preclinical cell therapy studies, we successfully differentiated hiPSC into RPE cells with phagocytic activity and developed a new differentiation protocol to obtain RPC expressing precursor

photoreceptor markers. We established that the best RPC developmental time window for transplantation in RCS rats at postnatal day 21 is days 45–75, as immature progenitors from an earlier stage (day 21) were unable to preserve retinal degeneration or visual function. Collectively, our data demonstrate for the first time that RPE cells and RPC in a combined therapy can preserve both endogenous photoreceptors and visual function in a manner superior to that using only RPE cells or RPC. The rationale for choosing a transplantation scheme combining RPE cells with RPC, both derived from hiPSC, was based on our previous study,[38] where we found that transplantation of RPE cells into the RCS rat model of severe photoreceptor degeneration, caused by RPE phagocytosis dysfunction, was unable to halt photoreceptor-degenerative processes and preserve visual function.

Several retinal cell types have been successfully transplanted into wild-type or degenerative animal models, and most were cells obtained from the neuroretinas of young animals.[28,42] These studies show that neuroretinal cells can survive for long periods in the host retina, integrate into the ONL, and mature as photoreceptors, forming synaptic connections with bipolar cells,[24] suggesting that the multipotent capacity of retinal progenitor cells is key to ensure the proper formation of retinal structures, making them valuable for retinal regeneration therapy. In terms of translating this approach to treat patients, fetal retinal tissue may present limitations, including tissue availability and ethical acceptability. Accordingly, derivation of retinal cells from hESC and hiPSC represents the most promising cell source for cell therapy. Several protocols have been used to generate photoreceptors in 2D cultures and 3D retinal organoids from both hESC and hiPSC,[23,28–30,33,43–46] yielding different populations of postmitotic cone and rod photoreceptor precursors. Our differentiation protocol in 2D yielded a population of RPC consisting of an assortment of postmitotic precursors and more mature photoreceptor cells at day 45 of differentiation. The expression profile of photoreceptor genes in our retinal RPC cultures is very similar to that recently reported by Mellough et al.[34] and reviewed by Llonch et al.,[47] who described the highest peak of hESC-derived photoreceptors expressing *OPSINSW* and *RHODOPSIN* between days 40 and 60 of differentiation. The failure of transplanted immature RPCs to survive in the host eye indicates that only postmitotic precursors may survive and integrate.[24] Indeed, we found that our retinal cells at day 21 of differentiation failed to exert a protective effect on host photoreceptors or visual function. In this line, the absence of mitotically active or undifferentiated cells is particularly important to prevent teratoma formations. Although the retinal progenitors at day 21 did not have any effect on host retinas, no neoplastic structures were evident, suggesting a postmitotic state of differentiated RPC from that stage onward in differentiation.

We optimized the *trans*-scleral route of administration, in the form of cell suspension, into the subretinal space of rat eyes to achieve high survival rates. This offers major advantages over other routes or cell sources: (1) it is technically easier and less traumatic than the *trans*-corneal route, the transplantation of RPE sheets, or retinal patches; (2) it allows the transplantation of an accurate cell number in a localized area; and (3) it enables a better isolation, characterization, and cryopreservation, as well as quality control of the transplantable cell type. For therapeutic applications, the capacity of grafted cells transplanted subretinally to functionally integrate into the host retina relies on their survival and migratory capacity.[48] In the majority of cases, however, this type of transplantation leads to a low number of cells integrating into the correct layer, thus limiting the effectiveness of the therapy. We show that although RPE cells and RPC survived up to 12 weeks in the subretinal space and mainly exerted protective effects on endogenous photoreceptors, only a low number RPC and RPE cells integrated into the correct layer. There are several possible explanations for this. First, RCS rats exhibit severe photoreceptor loss, but the RPE cell layer remains mostly intact. Accordingly, transplanted RPE cells may not have sufficient space to accommodate into the layer close to Bruch's membrane. Second, transplantation of RPC in retinas retaining endogenous photoreceptors may lead to low integration rates because of the presence of limiting membranes, as we showed at 1 week post-transplantation (Figure S4). Recent studies indicate that transplantation of cell suspensions into retinas lacking photoreceptors might be a better model to study photoreceptor engraftment and synaptic connectivity with host bipolar cells.[20,45] Other studies point toward the use of chemical modulators of glial response, such as matrix metalloproteinase 2 (MMP2) or aminoadipic acid, to reduce physical impairment of limiting membranes and to enhance donor retinal integration into the ONL[49–53]. Finally, transplantation of RPC into a neurodegenerative environment has several implications that can reduce transplanted cell survival and integration, such as gliosis, inflammation, and activated immune response.

Histological analyses of eyes transplanted with combined RPE + RPC revealed the preservation of retinal anatomy adjoining the engrafted area and the rescue of photoreceptors, which correlates well with the functional data. Of note, the fact that the area of photoreceptor rescue extended beyond the limits of the injection site suggests a non-cell-autonomous trophic effect of transplanted cells on the survival of host photoreceptors rather than their replacement. This was previously observed by others,[18,19] but the neuroprotective mechanism is still unknown. Previous work by Klassen et al.[54] found that mouse retinas transplanted with RPC showed preservation of host photoreceptors by a rescue mechanism that was not previously observed after intravitreal injections,[55] indicating that for cell rescue purposes, subretinal injections are more effective. In addition, material transfer between cells has been proposed as a new alternative mechanism in which retinal cells can benefit.[5] This novel concept is based on the exchange of cytoplasmic material between the engrafted retinal cells and the host photoreceptors. Previous reports observed that the nonphotoreceptor fraction of retinal progenitor cells presented limited capacity to integrate into the ONL upon transplantation and suggested that the material transfer observed from donor to host cells could be photoreceptor-photoreceptor specific.[24,46,56–58] This is in accordance with our results using the combined RPE + RPC therapy, where we observed some degree of material exchange with the rat retina,[31] likely

due to RPCs rather than the RPE, since this phenomenon was not evident in eyes injected with RPE cells alone. Thus, the fact that the combined therapy induced conservation of host ONL despite the minimal integration of transplanted RPC, in combination with some cytoplasmic transfer, suggests that the efficacy of the combined therapy is partially due to a neuroprotective effect rather than functional integration.

Conclusions

We show here the potential benefit of combined RPC and RPE cell therapy in the RCS rat model of retinitis pigmentosa. Cells not only survived in the host retina but also were able to delay disease progression and preserve visual function better than RPC or RPE therapies. In late-stage retinal degeneration, when the irreversible loss of photoreceptors leads to blindness, the combined hiPSC-derived RPC and RPE cell therapy might represent a more feasible and complete option for cell replacement than RPC or RPE therapy alone.

MATERIALS AND METHODS

Cell culture conditions

The hiPSC line CBiPS30-4F-5,[59] which was previously used to successfully generate RPE cells,[38] was obtained from the Spanish Stem Cell Bank upon Ethics Review Board and competent authority approval. Cells were cultured feeder free on Matrigel (Corning)-coated plates and expanded in chemically defined mTeSR1 medium (STEMCELL Technologies) at 37°C with 5% (v/v) CO_2. The medium was changed every other day until cells were ready for passaging. Colonies were detached using 0.5 mM EDTA (Thermo Fisher Scientific) for 2 min at room temperature.

hiPSC differentiation to RPE and RPCs

Differentiation of CBiPS30-4F-5 hiPSC to RPE cells was performed as described.[38] Briefly, hiPSC colonies on Matrigel (Corning)-coated plates were expanded in mTeSR1 medium (STEMCELL Technologies) until they reached 70% confluence. Retinal induction was performed by replacing mTeSR1 with RPE medium containing Dulbecco's modified Eagle's medium (DMEM): nutrient mixture F-12 (DMEM/F12; Gibco) with 10% knockout serum replacement (KSR; Gibco), 0.1 mM nonessential amino acids (Gibco), 1% N2 (Gibco), 2% B27 (Gibco), 0.1 μM dexamethasone (Sigma), 10 mM β-glycerophosphate (Sigma), 20 ng/mL human insulin growth factor (IGF)-1 (R&D Systems), and 10 mM nicotinamide (Sigma), which were replenished every other day. After 6 weeks of differentiation, visible pigmented foci were manually isolated and expanded in RPE medium on Matrigel-coated plates. For purification and expansion, RPE cultures were treated with 0.05% trypsin (Gibco) for 2 min to remove fibroblast-like cells, and then remaining attached RPE cells were disaggregated using 0.25% trypsin and cultured in monolayers. For all experiments, hiPSC-RPE cells expanded 2–4 times and were frozen in 10% DMSO in fetal bovine serum medium. Lentiviral transduction and cell characterization are described in Supplemental materials and methods.

Retinal differentiation was based on a published protocol[39] with slight modifications. When confluent, hiPSC colonies were dissociated into small clumps, and EBs were formed in conical-bottom 96-well plates in mTeSR1 medium (STEMCELL Technologies). After 48 h, EBs were transferred to low-attachment plates with retinal induction medium (RIM) containing DMEM: nutrient mixture F-12 (DMEM/F12; Gibco), 10% KSR (Gibco), 0.1 mM nonessential amino acids (Gibco), 1% N2 (Gibco), 2% B27 (Gibco), supplemented with 10 ng/mL Noggin (STEMCELL Technologies), 10 ng/mL DKK-1 (STEMCELL Technologies), 10 ng/mL IGF-1 (R&D Systems), and 5 ng/mL basic fibroblast growth factor (bFGF; Millipore). At day 5, EBs were plated onto Matrigel-coated plates (5–10 EBs per cm^2) to facilitate rapid conversion into retinal progenitors[43] and were maintained in RIM without KSR, which was changed every other day. To enrich for retinal progenitors, neural rosettes were manually picked and expanded on Matrigel-coated plates. From day 30, retinal progenitors were cultured in RIM without KSR, supplemented with 10 ng/mL IGF-1, 20 mM taurine, and 500 nM all-*trans* retinoic acid (Sigma) until the end of the protocol. In addition, 10 μM γ-secretase inhibitor, DAPT (Sigma), a Notch inhibitor, was added to media from days 28 to 32. Before day 45 of retinal differentiation, RPCs destined for subretinal injection were transduced with lentiviral particles carrying a GFP reporter gene (cell characterization is described in Supplemental materials and methods).

Animals

All procedures were approved by the Animal Care and Use Committee of the Vall d'Hebron Research Institute and were performed in accordance with the tenets of the European Community (86/609/CEE) and the Association for Research in Vision and Ophthalmology. Animals used were 21- to 24-day-old dystrophic (rdy2/p+) RCS rats, which were maintained on a 12-h light/dark cycle with *ad libitum* food and water. To avoid human cell graft rejection, animals were immunosuppressed by oral gavage with cyclosporin A 20 mg/kg/day (Novartis Pharma AG). Treatment was maintained throughout the entire experiment, starting 2 days before transplantation.

Surgery and transplantation

Before surgery, GFP-expressing differentiated RPE cells and RPCs were dissociated in TrypLE Select (Gibco), neutralized, and passed through a 70-μm filter to remove cell clumps. Cells suspended in serum-free DMEM/F12 medium at 5×10^4 cells/μL. Four groups of RCS rats were used for a single-cell injection (2 μL in total) into the subretinal space at postnatal days 21–24 as follows (see Table 1): group 1, transplantation of 100,000 RPE cells; group 2, cotransplantation of 50,000 RPE cells and 50,000 RPC mixture (note that in experiment #1, two additional animal groups were included for pilot studies of transplantation of RPE + RPC at different time points of the differentiation process to assess the best option); group 3, transplantation of 100,000 RPC at days 45−50; and group 4, injection of medium as a control (sham). Animals were anesthetized with a mixture of 2% isoflurane (Arrane; Baxter Laboratories)/1% O_2 and maintained with a rat nasal mask. Pupils were dilated with tropicamide (10 mg/mL Colircusi Tropicamida; Alcon Cusí Laboratories). Under a surgical microscope, simple sutures were performed in the upper eyelid and upper limbal conjunctiva with Prolene 7/0 Ethicon

(Johnson & Johnson) in order to expose the superior bulbar conjunctiva, and a 2-mm sclerotomy was performed using a 20G blade, 4 mm from the limbus. 2 μL of cell suspension was loaded into a 32G blunt needle attached to a 10-μL Nanofil syringe (World Precision Instruments), which was introduced tangentially into the subretinal space through the sclerotomy. Finally, the needle and securing sutures were carefully removed, and a drop of tobramycin and dexamethasone (Tobradex 3 mg/mL + 1 mg/mL; Alcon Cusí Laboratories) was topically administered just after surgery as a local anti-inflammatory and antibiotic prophylaxis. Those eyes that did not present an evident fluorescent bleb in the subretinal space assessed by fundus imaging and OCT were excluded from the study.

In vivo analyses

Animals were maintained over 12 weeks, and structural and functional analyses were performed periodically by FFI, OCT, and Ganzfeld ERG using the Micron III platform (Phoenix Research Laboratories). For all procedures, animals were anesthetized with inhaled 2% isofluorane and placed on a heating pad at 37°C. Pupils were dilated with a mixture of tropicamide and phenylephrine (100 mg/mL Colircusí Fenilefrina; Alcon Cusí Laboratories), and 2% Methocel gel (OmniVision) was administered to the cornea to favor contact with the lens.

Color fundus and fluorescent images were taken at the day of surgery and 1, 2, 4, 8, and 12 weeks postinjection using the Micron III imaging microscope (Phoenix Research Laboratories). RPE and RPC grafts were identified as green fluorescent spots in the eye fundus under the retina. Images from different time points in the same animal were compared to monitor the presence of the transplanted cells. Following FFI and with the animal still anesthetized, OCT images were taken by image-guided tomography (Micron IV-OCT2; Phoenix Research Laboratories). For each eye, the scanner was placed over the injected area, and three images were taken near the injection point. One image was also taken in a noninjected area at the opposite site of the eye. Finally, the images were analyzed with InSight 3D Voxeleron software for the quantitative assessment of whole retina thickness and the photoreceptor layer. The percentage of preservation of total retina thickness and photoreceptor layer thickness in Figure 4 was calculated by applying the following formula, using the values of a noninjected area and the injected area of the same eye:

$$\%\ \text{preservation} = \frac{(\text{injected area thickness}) - (\text{non injected area thickness})}{\text{non injected area thickness}} \times 100.$$

Functional responses of the retinas were recorded at 4, 8, and 12 weeks postinjection using the Phoenix Ganzfeld ERG system (Phoenix Research Laboratories). Dark-adapted rats (12–16 h) were anesthetized under dim red light, and pupils were dilated as described. Three electrodes were placed on the tail (ground electrode), the head (reference electrode), and the cornea, located in the objective lens (corneal electrode). Scotopic retinal responses were recorded using light flashes (1 ms duration, light intensities ranging from −1.1 to 1.9 log cd · s · m^{-2}, with 10 sweeps and 10- to 60-s intervals, depending on the intensity). Waveforms were analyzed using LabScribe ERG software (Phoenix Research Laboratories), and the a- and b-wave amplitudes and latencies were determined.

Histology and immunochemistry

RPE flat mounts

At 8 and 12 weeks postinjection, eyes were enucleated and dissected in PBS to remove cornea, lens, and retina. The posterior eyecups were fixed in 4% (w/v) paraformaldehyde (PFA) for 1 h, rinsed 3 times for 10 min with phosphate-buffered saline (PBS), and flattened by making four radial incisions. For detection of ZO-1, eyecups were subjected to immunochemistry, as described below.

Histology

At 1, 8, or 12 weeks postinjection, eyes were enucleated and fixed in 4% PFA overnight at 4°C. After 3 rinses with PBS, eyes were subjected to dehydration using a successive sucrose concentration as follows: 15% for 30 min, 20% for 60 min, and 30% overnight, all at 4°C. Eyes were embedded in optimum cutting temperature compound (Tissue-Tek), frozen, and stored at −80°C. Thin serial sections of 10 μm were cut using a Cryostat microtome (Leica) and collected on Superfrost glass slides. Transversal cryosections were stained with hematoxylin and eosin by standard protocols. Images were acquired on an FSX100 microscope (Olympus Life Sciences).

Immunohistochemistry

Cryosections and RPE flat mounts were washed in PBS and permeabilized and blocked in PBS containing 0.5% Triton X-100 and 6% normal donkey serum (NDS; Millipore) for 1 h at room temperature. Primary and secondary antibodies (see Table S2) were diluted in 0.1% Triton X-100 and 6% NDS in PBS and incubated in a humidified chamber overnight at 4°C or 2 h at 37°C, respectively. Slides were mounted in mounting medium containing 4′,6-diamidino-2-phenylindole (DAPI), and images were obtained on a DMI6000 confocal microscopy (Leica Microsystems).

Statistics

All quantitative data were analyzed using GraphPad Prism software (GraphPad Software). The unpaired two-tailed Student's t-test was applied to determine statistical significance between 2 groups. For more than 2 groups, 1- or 2-way ANOVA with a Tukey-corrected

post hoc test was used. Statistical significance was considered at <0.05 with a confidence interval of 95%.

SUPPLEMENTAL INFORMATION

Supplemental Information can be found online at https://doi.org/10.1016/j.omtm.2021.02.006.

ACKNOWLEDGMENTS

The authors thank Lola Mulero, Begoña Aran, and Bernd Kuebler (Core Facilities and Stem Cell Bank at P-CMR[C]-IDIBELL) for technical assistance. We thank CERCA Program/Generalitat de Catalunya for institutional support. Histological processing was performed by the ICTS-NANBIOSIS-U20/FVPR at the Vall d'Hebron Institute of Research (VHIR). The data that support the findings of this study are available in the Supplemental information. This research project was funded by grants from La Marató de TV3 Foundation (484/C/2012), PRB2-ISCIII-SGEFI- FEDER-PE I+D+i 2013-2016 (PT13/0001/0041), and ISCIII-FEDER RETICS (Oftared; RD16/0008).

AUTHOR CONTRIBUTIONS

Conception and design, collection and assembly of data, data analysis and interpretation, and manuscript writing, A.S., A.D., and L.F.; collection and assembly of data, D.M.R., A.B., B.F.-d.-S., M.A.Z., and A.R.; conception and design, financial support, and final approval of manuscript, A.V. and J.G.-A.; final approval of manuscript, A.D., A.V., and J.G.-A.

DECLARATION OF INTERESTS

The authors declare no competing interests.

REFERENCES

1. Pascolini, D., and Mariotti, S.P. (2012). Global estimates of visual impairment: 2010. Br. J. Ophthalmol. *96*, 614–618.
2. (1995). Simple anatomy of the retina. In Webvision: The Organization of the Retina and Visual System, H. Kolb, E. Fernandez, and R. Nelson, eds. (University of Utah Health Sciences Center).
3. Strauss, O. (2005). The retinal pigment epithelium in visual function. Physiol. Rev. *85*, 845–881.
4. Hamon, A., Roger, J.E., Yang, X.-J., and Perron, M. (2016). Müller glial cell-dependent regeneration of the neural retina: An overview across vertebrate model systems. Dev. Dyn. *245*, 727–738.
5. Gasparini, S.J., Llonch, S., Borsch, O., and Ader, M. (2019). Transplantation of photoreceptors into the degenerative retina: Current state and future perspectives. Prog. Retin. Eye Res. *69*, 1–37.
6. Zarbin, M., Sugino, I., and Townes-Anderson, E. (2019). Concise Review: Update on Retinal Pigment Epithelium Transplantation for Age-Related Macular Degeneration. Stem Cells Transl. Med. *8*, 466–477.
7. Schwartz, S.D., Regillo, C.D., Lam, B.L., Eliott, D., Rosenfeld, P.J., Gregori, N.Z., Hubschman, J.-P., Davis, J.L., Heilwell, G., Spirn, M., et al. (2015). Human embryonic stem cell-derived retinal pigment epithelium in patients with age-related macular degeneration and Stargardt's macular dystrophy: follow-up of two open-label phase 1/2 studies. Lancet *385*, 509–516.
8. Song, W.K., Park, K.-M., Kim, H.-J., Lee, J.H., Choi, J., Chong, S.Y., Shim, S.H., Del Priore, L.V., and Lanza, R. (2015). Treatment of macular degeneration using embryonic stem cell-derived retinal pigment epithelium: preliminary results in Asian patients. Stem Cell Reports *4*, 860–872.
9. Mandai, M., Watanabe, A., Kurimoto, Y., Hirami, Y., Morinaga, C., Daimon, T., Fujihara, M., Akimaru, H., Sakai, N., Shibata, Y., et al. (2017). Autologous Induced Stem-Cell-Derived Retinal Cells for Macular Degeneration. N. Engl. J. Med. *376*, 1038–1046.
10. Schwartz, S.D., Hubschman, J.-P., Heilwell, G., Franco-Cardenas, V., Pan, C.K., Ostrick, R.M., Mickunas, E., Gay, R., Klimanskaya, I., and Lanza, R. (2012). Embryonic stem cell trials for macular degeneration: a preliminary report. Lancet *379*, 713–720.
11. Arai, S., Thomas, B.B., Seiler, M.J., Aramant, R.B., Qiu, G., Mui, C., de Juan, E., and Sadda, S.R. (2004). Restoration of visual responses following transplantation of intact retinal sheets in rd mice. Exp. Eye Res. *79*, 331–341.
12. Ghosh, F., Wong, F., Johansson, K., Bruun, A., and Petters, R.M. (2004). Transplantation of full-thickness retina in the rhodopsin transgenic pig. Retina *24*, 98–109.
13. Aramant, R.B., and Seiler, M.J. (2002). Transplanted sheets of human retina and retinal pigment epithelium develop normally in nude rats. Exp. Eye Res. *75*, 115–125.
14. Silverman, M.S., Hughes, S.E., Valentino, T.L., and Liu, Y. (1992). Photoreceptor transplantation: anatomic, electrophysiologic, and behavioral evidence for the functional reconstruction of retinas lacking photoreceptors. Exp. Neurol. *115*, 87–94.
15. Liu, Y., Chen, S.J., Li, S.Y., Qu, L.H., Meng, X.H., Wang, Y., Xu, H.W., Liang, Z.Q., and Yin, Z.Q. (2017). Long-term safety of human retinal progenitor cell transplantation in retinitis pigmentosa patients. Stem Cell Res. Ther. *8*, 209.
16. Luo, J., Baranov, P., Patel, S., Ouyang, H., Quach, J., Wu, F., Qiu, A., Luo, H., Hicks, C., Zeng, J., et al. (2014). Human retinal progenitor cell transplantation preserves vision. J. Biol. Chem. *289*, 6362–6371.
17. Klassen, H., Kiilgaard, J.F., Warfvinge, K., Samuel, M.S., Prather, R.S., Wong, F., Petters, R.M., la Cour, M., and Young, M.J. (2012). Photoreceptor Differentiation following Transplantation of Allogeneic Retinal Progenitor Cells to the Dystrophic Rhodopsin Pro347Leu Transgenic Pig. Stem Cells Int. *2012*, 939801.
18. Cuenca, N., Fernández-Sánchez, L., McGill, T.J., Lu, B., Wang, S., Lund, R., Huhn, S., and Capela, A. (2013). Phagocytosis of photoreceptor outer segments by transplanted human neural stem cells as a neuroprotective mechanism in retinal degeneration. Invest. Ophthalmol. Vis. Sci. *54*, 6745–6756.
19. Tsai, Y., Lu, B., Bakondi, B., Girman, S., Sahabian, A., Sareen, D., Svendsen, C.N., and Wang, S. (2015). Human iPSC-Derived Neural Progenitors Preserve Vision in an AMD-Like Model. Stem Cells *33*, 2537–2549.
20. Collin, J., Zerti, D., Queen, R., Santos-Ferreira, T., Bauer, R., Coxhead, J., Hussain, R., Steel, D., Mellough, C., Ader, M., et al. (2019). CRX Expression in Pluripotent Stem Cell-Derived Photoreceptors Marks a Transplantable Subpopulation of Early Cones. Stem Cells *37*, 609–622.
21. Tucker, B.A., Park, I.-H., Qi, S.D., Klassen, H.J., Jiang, C., Yao, J., Redenti, S., Daley, G.Q., and Young, M.J. (2011). Transplantation of adult mouse iPS cell-derived photoreceptor precursors restores retinal structure and function in degenerative mice. PLoS ONE *6*, e18992.
22. Santos-Ferreira, T., Postel, K., Stutzki, H., Kurth, T., Zeck, G., and Ader, M. (2015). Daylight vision repair by cell transplantation. Stem Cells *33*, 79–90.
23. Lamba, D.A., Gust, J., and Reh, T.A. (2009). Transplantation of human embryonic stem cell-derived photoreceptors restores some visual function in Crx-deficient mice. Cell Stem Cell *4*, 73–79.
24. MacLaren, R.E., Pearson, R.A., MacNeil, A., Douglas, R.H., Salt, T.E., Akimoto, M., Swaroop, A., Sowden, J.C., and Ali, R.R. (2006). Retinal repair by transplantation of photoreceptor precursors. Nature *444*, 203–207.
25. Pearson, R.A., Barber, A.C., Rizzi, M., Hippert, C., Xue, T., West, E.L., Duran, Y., Smith, A.J., Chuang, J.Z., Azam, S.A., et al. (2012). Restoration of vision after transplantation of photoreceptors. Nature *485*, 99–103.
26. Singh, M.S., Charbel Issa, P., Butler, R., Martin, C., Lipinski, D.M., Sekaran, S., Barnard, A.R., and MacLaren, R.E. (2013). Reversal of end-stage retinal degeneration and restoration of visual function by photoreceptor transplantation. Proc. Natl. Acad. Sci. USA *110*, 1101–1106.

27. Lakowski, J., Gonzalez-Cordero, A., West, E.L., Han, Y.-T., Welby, E., Naeem, A., Blackford, S.J.I., Bainbridge, J.W.B., Pearson, R.A., Ali, R.R., and Sowden, J.C. (2015). Transplantation of Photoreceptor Precursors Isolated via a Cell Surface Biomarker Panel From Embryonic Stem Cell-Derived Self-Forming Retina. Stem Cells *33*, 2469–2482.

28. Lakowski, J., Baron, M., Bainbridge, J., Barber, A.C., Pearson, R.A., Ali, R.R., and Sowden, J.C. (2010). Cone and rod photoreceptor transplantation in models of the childhood retinopathy Leber congenital amaurosis using flow-sorted Crx-positive donor cells. Hum. Mol. Genet. *19*, 4545–4559.

29. Banin, E., Obolensky, A., Idelson, M., Hemo, I., Reinhardtz, E., Pikarsky, E., Ben-Hur, T., and Reubinoff, B. (2006). Retinal incorporation and differentiation of neural precursors derived from human embryonic stem cells. Stem Cells *24*, 246–257.

30. Barnea-Cramer, A.O., Wang, W., Lu, S.-J., Singh, M.S., Luo, C., Huo, H., McClements, M.E., Barnard, A.R., MacLaren, R.E., and Lanza, R. (2016). Function of human pluripotent stem cell-derived photoreceptor progenitors in blind mice. Sci. Rep. *6*, 29784.

31. Gonzalez-Cordero, A., Kruczek, K., Naeem, A., Fernando, M., Kloc, M., Ribeiro, J., Goh, D., Duran, Y., Blackford, S.J.I., Abelleira-Hervas, L., et al. (2017). Recapitulation of Human Retinal Development from Human Pluripotent Stem Cells Generates Transplantable Populations of Cone Photoreceptors. Stem Cell Reports *9*, 820–837.

32. Hambright, D., Park, K.-Y., Brooks, M., McKay, R., Swaroop, A., and Nasonkin, I.O. (2012). Long-term survival and differentiation of retinal neurons derived from human embryonic stem cell lines in un-immunosuppressed mouse retina. Mol. Vis. *18*, 920–936.

33. Lamba, D.A., McUsic, A., Hirata, R.K., Wang, P.-R., Russell, D., and Reh, T.A. (2010). Generation, purification and transplantation of photoreceptors derived from human induced pluripotent stem cells. PLoS ONE *5*, e8763.

34. Mellough, C.B., Sernagor, E., Moreno-Gimeno, I., Steel, D.H.W., and Lako, M. (2012). Efficient stage-specific differentiation of human pluripotent stem cells toward retinal photoreceptor cells. Stem Cells *30*, 673–686.

35. Gal, A., Li, Y., Thompson, D.A., Weir, J., Orth, U., Jacobson, S.G., Apfelstedt-Sylla, E., and Vollrath, D. (2000). Mutations in MERTK, the human orthologue of the RCS rat retinal dystrophy gene, cause retinitis pigmentosa. Nat. Genet. *26*, 270–271.

36. Ryals, R.C., Andrews, M.D., Datta, S., Coyner, A.S., Fischer, C.M., Wen, Y., Pennesi, M.E., and McGill, T.J. (2017). Long-term Characterization of Retinal Degeneration in Royal College of Surgeons Rats Using Spectral-Domain Optical Coherence Tomography. Invest. Ophthalmol. Vis. Sci. *58*, 1378–1386.

37. Perlman, I. (1978). Dark-adaptation in abnormal (RCS) rats studied electroretinographically. J. Physiol. *278*, 161–175.

38. Riera, M., Fontrodona, L., Albert, S., Ramirez, D.M., Seriola, A., Salas, A., Muñoz, Y., Ramos, D., Villegas-Perez, M.P., Zapata, M.A., et al. (2016). Comparative study of human embryonic stem cells (hESC) and human induced pluripotent stem cells (hiPSC) as a treatment for retinal dystrophies. Mol. Ther. Methods Clin. Dev. *3*, 16010.

39. Lamba, D.A., Karl, M.O., Ware, C.B., and Reh, T.A. (2006). Efficient generation of retinal progenitor cells from human embryonic stem cells. Proc. Natl. Acad. Sci. USA *103*, 12769–12774.

40. Adachi, K., Takahashi, S., Yamauchi, K., Mounai, N., Tanabu, R., and Nakazawa, M. (2016). Optical Coherence Tomography of Retinal Degeneration in Royal College of Surgeons Rats and Its Correlation with Morphology and Electroretinography. PLoS ONE *11*, e0162835.

41. Ortin-Martinez, A., Tsai, E.L.S., Nickerson, P.E., Bergeret, M., Lu, Y., Smiley, S., Comanita, L., and Wallace, V.A. (2017). A Reinterpretation of Cell Transplantation: GFP Transfer From Donor to Host Photoreceptors. Stem Cells *35*, 932–939.

42. Bartsch, U., Oriyakhel, W., Kenna, P.F., Linke, S., Richard, G., Petrowitz, B., Humphries, P., Farrar, G.J., and Ader, M. (2008). Retinal cells integrate into the outer nuclear layer and differentiate into mature photoreceptors after subretinal transplantation into adult mice. Exp. Eye Res. *86*, 691–700.

43. Boucherie, C., Mukherjee, S., Henckaerts, E., Thrasher, A.J., Sowden, J.C., and Ali, R.R. (2013). Brief report: self-organizing neuroepithelium from human pluripotent stem cells facilitates derivation of photoreceptors. Stem Cells *31*, 408–414.

44. Eiraku, M., Takata, N., Ishibashi, H., Kawada, M., Sakakura, E., Okuda, S., Sekiguchi, K., Adachi, T., and Sasai, Y. (2011). Self-organizing optic-cup morphogenesis in three-dimensional culture. Nature *472*, 51–56.

45. Mandai, M., Fujii, M., Hashiguchi, T., Sunagawa, G.A., Ito, S.-I., Sun, J., Kaneko, J., Sho, J., Yamada, C., and Takahashi, M. (2017). iPSC-Derived Retina Transplants Improve Vision in rd1 End-Stage Retinal-Degeneration Mice. Stem Cell Reports *8*, 1112–1113.

46. Santos-Ferreira, T., Llonch, S., Borsch, O., Postel, K., Haas, J., and Ader, M. (2016). Retinal transplantation of photoreceptors results in donor-host cytoplasmic exchange. Nat. Commun. *7*, 13028.

47. Llonch, S., Carido, M., and Ader, M. (2018). Organoid technology for retinal repair. Dev. Biol. *433*, 132–143.

48. Warre-Cornish, K., Barber, A.C., Sowden, J.C., Ali, R.R., and Pearson, R.A. (2014). Migration, integration and maturation of photoreceptor precursors following transplantation in the mouse retina. Stem Cells Dev. *23*, 941–954.

49. Ma, J., Kabiel, M., Tucker, B.A., Ge, J., and Young, M.J. (2011). Combining chondroitinase ABC and growth factors promotes the integration of murine retinal progenitor cells transplanted into Rho(-/-) mice. Mol. Vis. *17*, 1759–1770.

50. Yao, J., Tucker, B.A., Zhang, X., Checa-Casalengua, P., Herrero-Vanrell, R., and Young, M.J. (2011). Robust cell integration from co-transplantation of biodegradable MMP2-PLGA microspheres with retinal progenitor cells. Biomaterials *32*, 1041–1050.

51. Suzuki, T., Mandai, M., Akimoto, M., Yoshimura, N., and Takahashi, M. (2006). The simultaneous treatment of MMP-2 stimulants in retinal transplantation enhances grafted cell migration into the host retina. Stem Cells *24*, 2406–2411.

52. Yu, W.-Q., Eom, Y.S., Shin, J.-A., Nair, D., Grzywacz, S.X.Z., Grzywacz, N.M., Craft, C.M., and Lee, E.-J. (2016). Reshaping the Cone-Mosaic in a Rat Model of Retinitis Pigmentosa: Modulatory Role of ZO-1 Expression in DL-Alpha-Aminoadipic Acid Reshaping. PLoS ONE *11*, e0151668.

53. Johnson, T.V., Bull, N.D., and Martin, K.R. (2010). Identification of barriers to retinal engraftment of transplanted stem cells. Invest. Ophthalmol. Vis. Sci. *51*, 960–970.

54. Klassen, H.J., Ng, T.F., Kurimoto, Y., Kirov, I., Shatos, M., Coffey, P., and Young, M.J. (2004). Multipotent retinal progenitors express developmental markers, differentiate into retinal neurons, and preserve light-mediated behavior. Invest. Ophthalmol. Vis. Sci. *45*, 4167–4173.

55. Eberle, D., Kurth, T., Santos-Ferreira, T., Wilson, J., Corbeil, D., and Ader, M. (2012). Outer segment formation of transplanted photoreceptor precursor cells. PLoS ONE *7*, e46305.

56. Pearson, R.A., Gonzalez-Cordero, A., West, E.L., Ribeiro, J.R., Aghaizu, N., Goh, D., Sampson, R.D., Georgiadis, A., Waldron, P.V., Duran, Y., et al. (2016). Donor and host photoreceptors engage in material transfer following transplantation of post-mitotic photoreceptor precursors. Nat. Commun. *7*, 13029.

57. Decembrini, S., Martin, C., Sennlaub, F., Chemtob, S., Biel, M., Samardzija, M., Moulin, A., Behar-Cohen, F., and Arsenijevic, Y. (2017). Cone Genesis Tracing by the Chrnb4-EGFP Mouse Line: Evidences of Cellular Material Fusion after Cone Precursor Transplantation. Mol. Ther. *25*, 634–653.

58. Singh, M.S., Balmer, J., Barnard, A.R., Aslam, S.A., Moralli, D., Green, C.M., Barnea-Cramer, A., Duncan, I., and MacLaren, R.E. (2016). Transplanted photoreceptor precursors transfer proteins to host photoreceptors by a mechanism of cytoplasmic fusion. Nat. Commun. *7*, 13537.

59. Giorgetti, A., Montserrat, N., Aasen, T., Gonzalez, F., Rodríguez-Pizà, I., Vassena, R., Raya, A., Boué, S., Barrero, M.J., Corbella, B.A., et al. (2009). Generation of induced pluripotent stem cells from human cord blood using OCT4 and SOX2. Cell Stem Cell *5*, 353–357.